Centrifugal-Barrier Effects in Resonance Partial Decay Widths, Shapes, and Production Amplitudes*

Frank von Hippel†
High Energy Physics Division, Argonne National Laboratory, Argonne, Illinois 60439

and

C. Quigg‡
Institute for Theoretical Physics, State University of New York, Stony Brook, New York 11790
(Received 16 September 1971)

(1) We review the experimental status of identifiable centrifugal-barrier effects in: (i) shapes of resonances, (ii) accounting for deviations in SU(2) and SU(3) predictions for ratios between partial decay widths, and (iii) accounting for the dependence on spin of the elastic widths of resonances lying on the same Regge trajectory. (2) We present a contour plot from which the "kinematic partial width" (centrifugal-barrier penetration factor times two-body phase space) of any resonance into any decay channel may be obtained immediately, given the orbital angular momentum, semiclassical impact parameter, and an assumed strong-interaction radius. Using this technique we display, as an example, the kinematically preferred decays of the high-spin mesons on the leading meson trajectory (assumed linear). (3) We obtain an approximate lower bound on the strong-interaction radius on the basis of general considerations. (4) We show that, for high-spin resonances, it can be expected that the mass enhancements in different decay channels associated with these resonances may be shifted by a half-width or so with respect to each other, because of different centrifugal-barrier effects in the different channels. (5) We also show that production cross sections of high-spin particles on leading linear trajectories by either formation or peripheral processes will be substantially suppressed by centrifugal-barrier effects. (6) Finally, we observe that the production cross sections and decay widths of mesons on the leading trajectory of the Veneziano model can be understood almost entirely on the basis of kinematical considerations if the radius of the region in which the decay particles interact strongly grows linearly with the mass of the decaying resonance.

I. INTRODUCTION

It is a familiar fact that, near threshold, resonance shapes and partial widths are influenced in characteristic ways by "centrifugal-barrier effects." For fixed-channel orbital angular momentum L these effects are correlated in a simple way with the semiclassical impact parameter,

$$b=[L(L+1)]^{1/2}/q, \tag{1.1}$$

where q is the channel wave number. When b is large (q small), cross sections and partial decay widths are relatively suppressed "other things being equal." This is the way in which we account for the apparent suppression of elastic resonances on their low-energy sides (see, e.g., Fig. 1) and for the direction in which most branching ratios into channels with $L\neq 0$ deviate from SU(2) or SU(3) predictions (see, e.g., Table I).

It has been suggested that centrifugal-barrier effects may also be important in the decays of high-mass, high-spin resonances.[1] If the spins of the resonances on the leading Regge trajectories are linear in mass squared,

$$J=\alpha' M^2+\alpha_0, \tag{1.2}$$

the growing ratio of J to mass at high masses will result in a corresponding growth of the impact parameters in all the decay channels with a consequent decrease in partial widths being expected.

Depending upon the assumed dependence on b and L of the centrifugal-barrier suppression effect, one expects the partial widths to decrease more or less rapidly. We are aware of two models,[2,3] both of which predict that the decrease will be rapid enough so that the total width will also decrease. Although both models consider explicitly only two-body (and quasi-two-body) decays, it might be hoped that many-particle decays would not change the qualitative results.

There are quantitative differences between the predictions of the two models, however. One, based on the assumption that two-particle interactions are negligible outside a fixed "interaction radius" R, leads to the prediction that total widths should fall exponentially roughly as[2]

$$\Gamma_{\text{tot}}\sim[(J/c)\ln(J/c)]^{-2\mu\sqrt{\alpha' J}}, \tag{1.3a}$$

where c is a constant estimated to have a value of

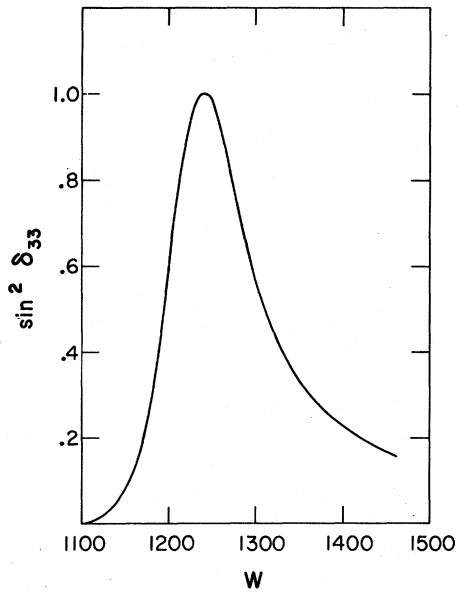

FIG. 1. Plot of $\sin^2\delta_{33}$ for π-N scattering against c.m. energy in MeV. Note the relative suppression of the low side of the resonance by "centrifugal-barrier effects." (Phase shifts are taken from Ref. 10. There is little discrepancy between the various solutions quoted for δ_{33} in this energy region.)

about 6, μ is the pion mass, and α' is the slope of the leading Regge trajectories. The other, the Veneziano model, leads to total widths decreasing only slightly more rapidly than[3]

$$\Gamma_{\text{tot}} \sim 1/\sqrt{J}\,. \tag{1.3b}$$

There is at present no agreement as to the *experimental* trend of resonance widths as a function of J.

In this paper, we will discuss the status of our understanding of centrifugal-barrier effects in elementary-particle physics. We use the general approach first applied more than twenty years ago to the neutron widths of low-lying excited states of nuclei by Feshbach, Peaslee, and Weisskopf.[4] This approach is based simply on the exponential decrease of the strong interactions outside of a certain separation distance in a two-body channel.

In order for centrifugal-barrier effects to be significant in comparison with unknown dynamical effects, the "interaction radius," outside of which the strong interactions are negligible in comparison to kinetic energy and/or centrifugal-barrier effects, must be significantly smaller than the semiclassical impact parameter associated with the channel orbital angular momentum and wave number.

In Sec. II we discuss the relationship between the interaction radius and resonance partial width and shapes. We also establish a lower bound on the interaction radius which depends on the partial decay widths.

In Sec. III we discuss those decay modes of the resonances on the leading nonstrange-meson trajectory (assumed linear) which are preferred on the basis of centrifugal-barrier considerations. We also compare the Veneziano-model results with the corresponding centrifugal-barrier expectations.

In Sec. IV we show that, in the case of high-spin resonances which decay into a number of two-body channels, the resonance "bump" will usually be shifted in some channels relative to its location in others because of different centrifugal-barrier effects in the different channels.

Finally, in Sec. V, we discuss on the basis of centrifugal-barrier considerations what resonances we expect to be able to produce most easily in formation experiments using real and virtual targets. Here again, we compare our results with Veneziano-model results.

II. THE INTERACTION RADIUS

In any two-body resonance decay channel (n) with orbital angular momentum $L \neq 0$, the form of the radial wave function will be determined dominantly by the repulsive centrifugal barrier and the channel wave number (q_n) for a particle separation (r)

TABLE I. Examples of apparent centrifugal-barrier effects on partial widths.

Decays	Impact parameters (F)	Experimental ratio of $M\Gamma_n/q_n$ [a]	Symmetry prediction	Constraint on the interaction radius
$\phi(1019) \to K_L K_S$	2.58	0.88 ± 0.11	1, SU(2)	almost none
$\to K^+K^-$	2.23			
$K^*(892) \to K\pi$	0.97	0.58 ± 0.09	0.75, SU(3)	$R < 1$ F
$\rho(765) \to \pi\pi$	0.78			

[a] Γ_n is the experimental partial width, q_n is the channel momentum. Partial widths are taken from Ref. 8. M is the mass of the decaying meson.

greater than a certain "interaction radius" (R). The approximate wave equation which holds outside R is

$$\frac{\partial^2}{\partial \rho^2} U_L^n(\rho) \cong \left(\frac{b_n^2}{r^2} - 1\right) U_L^n(\rho), \tag{2.1}$$

where

$$\rho \equiv q_n r$$

and

$$b_n = [L(L+1)]^{1/2}/q_n \tag{2.2}$$

is the semiclassical impact parameter.

The solution of (2.1), which has outgoing-wave boundary conditions appropriate to a decaying resonance, is proportional to a spherical Hankel function,

$$U_L^n(\rho) \underset{r>R}{\cong} iC_n \rho h_L^{(1)}(\rho) \underset{\rho \to \infty}{\sim} C_n \exp[i(\rho - \tfrac{1}{2} L\pi)], \tag{2.3}$$

where C_n is a constant which will be chosen below. In the Appendix we present a few relevant properties of the spherical Hankel functions.

Consider the situation if R is substantially less than b: For $r < b$, the radial probability density grows rapidly with decreasing r. The reason is, of course, that the outward-going wave is being reflected inward by the centrifugal barrier. At $r = R$, the radial probability density is

$$[T_L^n(R/b)]^{-1} \equiv \rho^2 |h_L^{(1)}(\rho)|^2, \quad r = R \tag{2.4}$$

times that at infinity. Since it requires this much probability density at R to "push" one unit of probability density to infinity, it would seem reasonable to define T_L^n as the "transmission coefficient" for the barrier outside of R.[5]

Kinematic Widths

If there is a fairly sharp separation at R between an "outer" region where the interactions are unimportant in comparison with the centrifugal barrier and an "inner" region where they dominate, one can factor T_L^n out of the partial decay width as an approximate representation of the centrifugal-barrier effects. To obtain a "reduced width" γ_n we also take the factor (q_n/M) out of the physical partial width Γ_n,

$$\Gamma_n = \gamma_n (q_n/M) T_L^n(R/b_n). \tag{2.5}$$

Here M is the mass of the decaying resonance and the factor (q_n/M) takes into account the variations of two-body phase space.[5]

Equation (2.5) represents an attempt, using the sharp-interaction-radius assumption, to separate the unknown dependence of Γ_n on the "dynamics" within the interaction region from the well-understood "kinematical" effects due to phase space and the centrifugal barrier outside R. The hope is, of course, that in some cases the variation of γ_n with L and R/b may be unimportant in comparison to that of $T_L^n(R/b)$, and that some of the gross variations of experimental partial widths might therefore be explained and even predicted primarily on the basis of kinematical considerations.

In Fig. 2(a), we display a contour plot of MR times the "kinematic width" Γ_n obtained by setting $\gamma_n = 1$ in (2.5) as a function of L and R/b. In Fig. 2(b), we display the same quantity as a function of the single variable R/b for various values of L. It will be seen from either plot that the kinematic width decreases very rapidly for either increasing L or decreasing R/b. With increasing L at fixed R/b we see the approach to the classical limit in which the wave function does not penetrate the increasingly high centrifugal barrier within the impact parameter. With decreasing R/b at fixed L, we see the suppression due to the increasing width (and height) of the centrifugal barrier which must be penetrated.

In Fig. 3, we plot M times the kinematic partial widths for the decays of the recurrences of the $\Delta(1236)$ and the $N(1520)$ into the $N\pi$ channel as a function of L for interaction radii of 0.7, 0.8, and 0.9 F. We normalize to unity at $L = 1$. On the same plot we give the experimental partial widths with the same normalization. The value of $R = 0.8$ F obtained in this application is comparable to the same value obtained for the "absorption radius" in an optical-model fit to $\pi^+ p$ scattering.[6] This plausible value of R obtained from a fit of the gross dependence of the partial widths on J therefore makes it possible to entertain an explanation that this variation is primarily due to "kinematic" effects. (Remember, however, that this conclusion depends entirely upon the identification of the bumps in the total cross sections above 2.5 GeV with the recurrences.[7])

It would be nice to have an independent estimate of the interaction radius compared with the estimate of 0.8 F obtained in one case above. We have looked at two possible sources of information: (i) resonance shapes, and (ii) deviations from SU(2) and SU(3) predictions of ratios between related partial widths.

Resonance Shapes

In this approach one assumes that the deviations of a resonance shape from a pure s-wave Breit-Wigner form are due to the kinematical factors in Eq. (2.5). One constructs an energy-dependent width function for each channel by neglecting the energy dependence of γ_n across the resonance,[8]

$$\Gamma_n(q_n) = \Gamma_n^0 \frac{(q_n/W)T_L^n(R/b_n)}{(q_n^0/M)T_L^n(R/b_n^0)}\,, \tag{2.6}$$

where W is the c.m. energy, q_n^0 and b_n^0 are, respectively, the values of the channel momentum and impact parameter at resonance, and Γ_n^0 is the energy-independent width. The energy-dependent widths are then inserted into the multichannel Breit-Wigner amplitude

$$T_{fi}^{\mathrm{BW}} = \frac{M(\Gamma_f\Gamma_i)^{1/2}}{M^2 - s - iM\Gamma_T}\,, \qquad \Gamma_T \equiv \sum_n \Gamma_n\,, \tag{2.7}$$

where the parameter R is varied to get a best fit to the observed resonance shape in the reaction in question.

Experimentally, the resonance with the best known shape, uncomplicated by inelastic channels, is the $\Delta(1236)$. Equations (2.6) and (2.7) *do not* provide a successful parametrization of this shape for any value of R. Thus, while a plausible value of $R = 1$ F gives a reasonable fit to the low-energy side of the curve shown in Fig. 1, we require a value of R of the order of 10 F to fit the high-energy side.[9] Similarly, there is little evidence for centrifugal-barrier enhancement on the high side of other resonances whose shapes are well known [e.g., the $\Lambda(1520)$ and the $\rho(765)$]. In the case of the $\Delta(1236)$, at least, it would appear therefore that the variation of γ_n on the high-energy side of the resonance is non-negligible. One possible reason why this should be so is related to the fact that there may be another P_{33} resonance[10] in the same channel at a mass of about 1690 MeV. If we assume that the resonances appear in the same eigenchannel, parametrize the resonant amplitude in terms of an eigenphase shift $\delta_{\mathrm{res}}(s)$, and project onto particular initial and final channels, we have

$$(T_{\mathrm{res}})_{fi} = X_f(s)X_i(s)\exp[i\delta_{\mathrm{res}}(s)]\sin[\delta_{\mathrm{res}}(s)]$$
$$= \frac{X_f(s)X_i(s)}{\cot\delta_{\mathrm{res}}(s) - i}\,. \tag{2.8}$$

It will be seen that, when δ_{res} passes through π between resonances, the denominator of (2.8), unlike that of (2.7), will have an infinity with the resonant amplitude having a corresponding zero. This zero would, of course, suppress any enhancement by centrifugal-barrier effects between the resonances. The fact that the P_{33} amplitude becomes very small above 1500 MeV might, therefore, be explained in

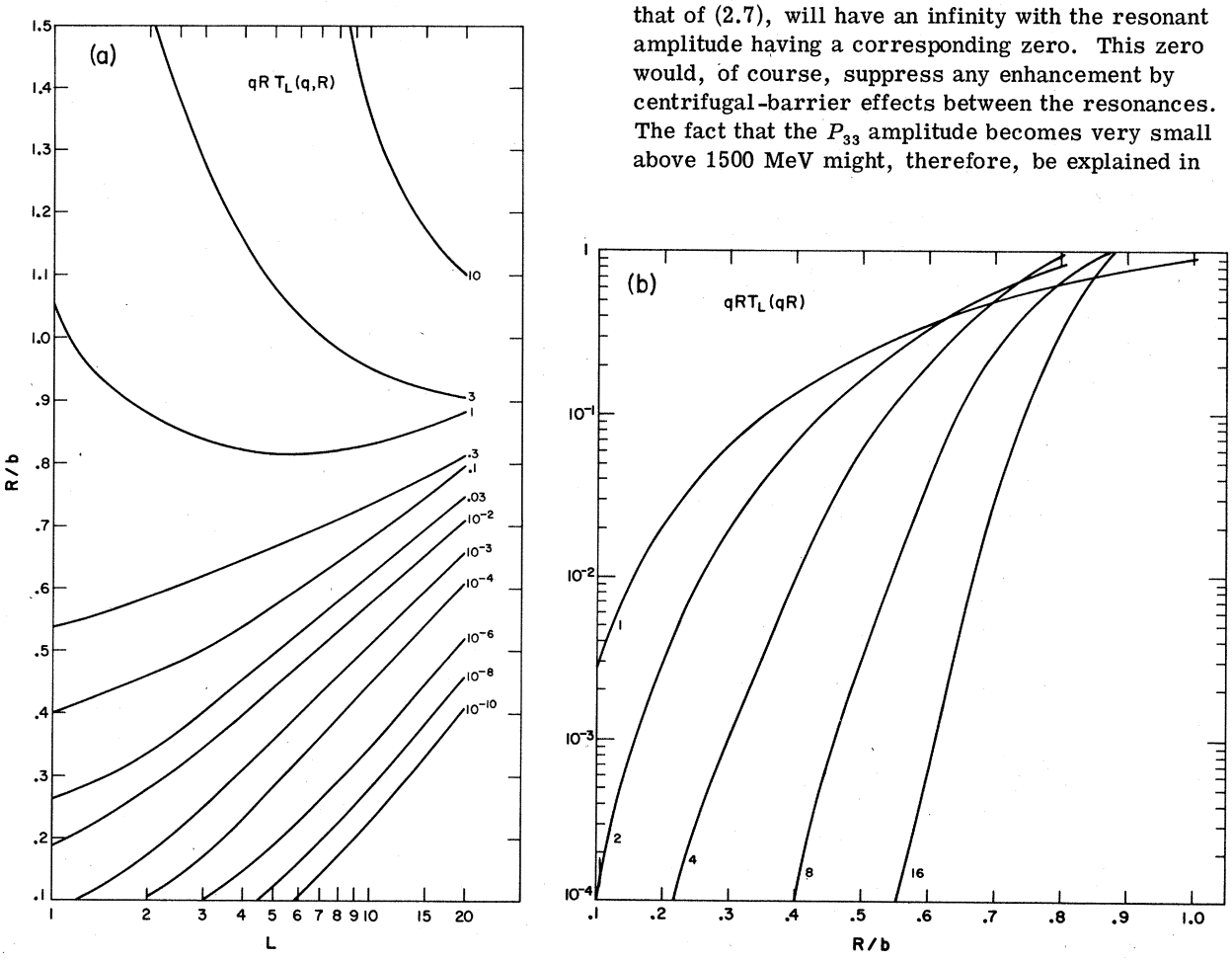

FIG. 2. Plot of MR times the "kinematic width" for a sharp interaction radius: (a) as a contour plot against L and R/b; (b) as a function of R/b for various L.

this way. (What we interpret here as a zero, due to the cycling of an eigenphase shift through π, might also be described in an N/D formulation as due to a Castillejo-Dalitz-Dyson pole.[11])

Whatever the reason for the failure of the parametrization (2.6), (2.7) we must obviously look elsewhere for a believable estimate of the interaction radius R.

Deviations from SU(2) or SU(3) Predictions

One possible mechanism for breaking SU(2) or SU(3) predictions for the ratios between partial decay widths would be to have the symmetry breaking occur entirely in the kinematical factor of (2.5) and not in γ_n. The symmetry breaking would then be entirely due to the deviations from equality of the c.m. momenta in the different channels related by SU(3). In Table I, we have seen examples of symmetry breaking which are in the direction suggested by this mechanism. One might hope that a fit of the experimental ratios to this hypothesis would then give a value for the interaction radius R.

Unfortunately, experimental partial widths do not seem to be well enough determined at present to provide a stringent test of this hypothesis or more than an upper bound on R. The deviation from the SU(2) prediction of unity for the ϕ branching ratio in Table I hardly restricts the value of R at all. Because of the larger ratio between channel momenta in SU(3), the results are more stringent, however: The ratio between K^* and ρ partial widths on Table I gives 1.0 F as an upper bound on R. Probably the most one can say with confidence is that the current status of the predictions of SU(3) is reasonably consistent with any interaction radius less than 1.0 F although a smaller radius seems to be preferred.[12]

Lower Bound on R

Above we have seen the hypothesis expressed in (2.5); that, in any resonance decay channel with $L \neq 0$, there is a fairly well-defined interaction radius outside of which the behavior of the channel wave function is affected strongly by the centrifugal barrier and relatively weakly by strong interactions between the decay products. (This subsumes the assumption that the interaction radius is comparable to or smaller than the impact parameter.) The hypothesis was supplemented with additional assumptions in order to predict two classes of relationships between partial decay widths: (i) It was assumed that γ_n was varied slowly from resonance to resonance along a Regge trajectory. The resulting hypothesis gave a reasonable description of what indications we have of the variation of the partial widths into the πN channel along the $\Delta(1236)$ and $N(1520)$ trajectories with an interaction radius of about 0.8 F. (ii) It was assumed, for resonance decay amplitudes which would be related by SU(3) Clebsch-Gordan coefficients in the limit of SU(3) symmetry, that the symmetry relationships remain exact between the corresponding γ_n in the physical world of broken SU(3), i.e., all the symmetry breaking appears in the kinematic factors associated with the breaking of the SU(3) degeneracies of the particle masses. This hypothesis is in reasonable agree-

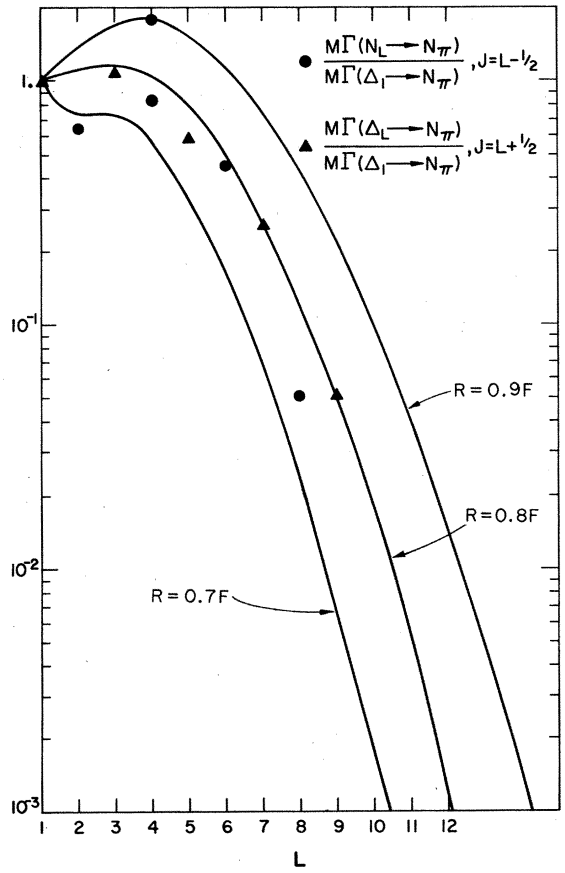

FIG. 3. Plot of M times the "kinematic" partial widths for the decays of the recurrences of the $\Delta(1136)$ and $N(1520)$ into the $N\pi$ channel as a function of L for various interaction radii. The solid triangles (circles) correspond to the "experimental" values obtained from Ref. 8 by assuming that the total πN cross-section bumps at $W = 2420$, 2850, and 3230 MeV ($W = 2650$ and 3030 MeV) are entirely due to the Regge recurrences of the $\Delta(1236)$ ($N(1520)$). Because of the systematic uncertainties of this assumption we give no errors. We have made the approximation (good for $L > 2$) that the trajectories are degenerate in L [i.e., the $N(1520)$ trajectory is one unit down from the $\Delta(1236)$ trajectory in J].

ment with experiment for any interaction radius less than about 1.0 F.

In this subsection, we complete our discussion of what we can say at present about the interaction radius (assuming that it continues to be a useful concept) by establishing, on rather general theoretical grounds, a lower bound on the interaction radius in any particular resonance decay channel with $L \neq 0$ in terms of the experimental partial decay width into that channel. This is a useful result because we do not understand the dynamical origin of resonances sufficiently to say that R must be larger than a certain value. The quark model, for example, would decouple these dynamics rather completely from the dynamics of ordinary particle exchanges whose effects are observed in peripheral interactions at high energies.

We begin by taking the impact parameter b as the separation point between the internal wave function of the resonance and the region where the wave function describes mostly the outgoing wave from its decay. The basis for our choice is that, for $R < b$, the wave function is dominantly of standing-wave form, i.e., is hardly distinguishable from a bound state with almost equal amounts of probability flowing outward and inward. We will choose the normalization constant C_n in (2.3) as

$$C_n = (\Gamma_n/v)^{1/2}, \tag{2.9}$$

so that the outward flux through a sphere associated with a large separation of the decay particles is equal to the partial width into the channel Γ_n. Here v is the relative particle velocity in the c.m. frame in channel n,

$$v = \frac{\partial W}{\partial q},$$

and q and W are, respectively, the c.m. momentum and energy in channel n evaluated at the resonance mass.

The total probability in the resonant state cannot exceed unity. The probability in the decay channel n between R and b_n,

$$\int_{q_n R}^{q_n b_n} |U_L^n(\rho)|^2 \frac{d\rho}{q_n} = \frac{\Gamma_n}{2 q_n v}\left[\rho^3 |h_L^{(1)}(\rho)|^2 - \rho^3 \,\mathrm{Re}\, h_{L+1}^{(1)}(\rho) h_{L-1}^{(1)*}(\rho)\right]_{q_n R}^{q_n b_n}, \tag{2.10}$$

must therefore be bounded by unity.

When one applies this condition to the decays of various established resonances one gets the results shown in Table II. These results, along with the results from analyses of the partial widths related by SU(3), establish as plausible interaction radii ranging from 0.25 to 0.75 F for the strong meson resonance decays and from 0.5 to 1 F for the strong baryon decays.

III. AN EXAMPLE OF "KINEMATIC SELECTION RULES"

It will be seen from Fig. 2(a) that one need know only the orbital angular momentum, semiclassical impact parameter, and interaction radius in a resonance decay channel to be able to read off MR times the corresponding kinematic width. In this section we will illustrate the ease with which one may understand the dependence of the kinematic width on decay channel through the use of this figure. We use it to establish the two-body and quasi-two-body decay modes of the mesons on the leading nonstrange trajectory which are preferred on the basis of centrifugal-barrier considerations. We will assume in this example that the mass squared of the resonances on this (ρ, A_2, ω, f) trajectory is linear as a function of the resonance spin up to a spin of 20 (mass = 4.8 GeV/c^2). We will also assume an interaction radius of 0.5 F. Nonlinear trajectories or a different interaction radius may prove to be more appropriate at some later time. For example, from a comparison with Veneziano-model results below, we find that the interaction radius in the Veneziano model appears to increase along the leading trajectory

TABLE II. Lower bounds on the interaction radii for some particular decays.

Decay	Partial width (MeV)	L	Impact parameter (F)	Lower bound on R (F)
$\rho(765) \to \pi\pi$	120	1	0.78	0.1
$\phi(1019) \to K\bar{K}$	4	1	2.4	0.1
$f(1265) \to \pi\pi$	150	2	0.78	0.2
$\Delta(1236) \to N\pi$	120	1	1.21	0.4
$\Delta(1950) \to N\pi$	90	3	0.92	0.4
$\Delta(3230) \to N\pi$	2.2	9	1.00	0.5

roughly in proportion to the mass of the resonance. The reader may obtain results corresponding to his favored assumptions by making appropriate changes in the simple calculations which we make in this section. He may of course go through the analogous procedure to find the kinematically preferred decay modes of resonances on lower-lying meson trajectories or of resonances on baryon trajectories. Thus, our discussion here should be taken primarily as an illustration of the simplicity of the procedure by which such kinematical predictions can be obtained.

We have chosen to consider the decays of high-spin nonstrange meson resonances because these particles have the most angular momentum per unit mass and therefore have the best chance of being relatively narrow and separable from background. We are also, of course, motivated by historical reasons: The CERN missing-mass spectrometer results[13] indicate a rich spectrum of charged narrow nonstrange meson resonances up to a mass of 3.5 GeV/c^2. These missing-mass peaks appear to include obvious candidates for the recurrences of the ρ and A_2 on an exchange-degenerate trajectory linear in mass squared up to about spin 8,

$$M^2 = (J - \alpha_0)M_0^2. \tag{3.1}$$

It has been suggested that the narrowness of these mesons might be accounted for by centrifugal-barrier considerations such as those discussed here.[14] It should be emphasized, however, that at the time of this writing there is by no means agreement among experimentalists on the existence of narrow high-spin mesons on the leading trajectory. If these mesons are wide, the trajectory will depart from linearity. Also, there will be additional complexities in discussions of the decay schemes of these mesons if successive resonances on the leading trajectory are wide enough to overlap with each other.[15]

For reasons which will become clear below, we will consider as decay products primarily mesons on the $I=0,1$ leading natural- and unnatural-parity degenerate trajectories with the approximate trajectory parameters indicated.

$$\begin{aligned} &\mathfrak{L}^N(\rho, A_2, \omega, f): \quad \alpha_0^N = 0.485, \\ &\mathfrak{L}^U(\pi, A_1): \quad\quad\ \alpha_0^U = -0.02, \\ &M_0 = 1.054\ \text{GeV}/c^2. \end{aligned} \tag{3.2}$$

We consider the decays of the resonances on the $\mathfrak{L}^N$ trajectory. A resonance on the leading natural-parity trajectory will be denoted by $\mathfrak{L}_J^N$, where J denotes its angular momentum. Similarly, a resonance on the leading unnatural-parity trajectory will be denoted by $\mathfrak{L}_J^U$. We will only specify the isospin of a resonance when it makes a difference.

Consider the decay of a resonance with spin, parity, and mass J, P, and M on one linear Regge trajectory into a pair of resonances with spins, parities, and masses J_i, P_i, and M_i $(i=1,2)$ each of which lies on another linear trajectory. Angular momentum and parity conservation requires that the orbital angular momentum in the decay channel be at least

$$L_{\min} = J - J_1 - J_2 \quad \text{if } PP_1P_2 = (-)^{J+J_1+J_2}, \tag{3.3a}$$

$$L_{\min} = J - J_1 - J_2 + 1 \quad \text{if } PP_1P_2 = -(-)^{J+J_1+J_2}. \tag{3.3b}$$

The c.m. momentum in the decay channel will be

$$q = \{[(M^2 - M_1^2 - M_2^2)^2 - 4M_1^2M_2^2]/4M^2\}^{1/2}. \tag{3.4}$$

Assuming that the trajectories have the same slope and using (3.3), we may write (3.4) as

$$\frac{q}{M_0} = \left(\frac{[L_{\min} - (0,1) - (\alpha_0 - \alpha_0^2 - \alpha_0^1)]^2 - 4(J_1 - \alpha_0^1)(J_2 - \alpha_0^2)}{4(J - \alpha_0)}\right)^{1/2}. \tag{3.5}$$

Here the α_0's correspond to the intercepts of the Regge trajectories associated with the particles, $(M_0)^{-2}$ corresponds to their common slope, and (0, 1) corresponds to (3.3a) and (3.3b), respectively.

Combining (3.3) and (3.5) we obtain the minimum impact parameter b in the decay channel,

$$M_0 b = \left(\frac{4L_{\min}(L_{\min}+1)(J - \alpha_0)}{[L_{\min} + \alpha_0^1 + \alpha_0^2 - \alpha_0 - (0,1)]^2 - 4(J_1 - \alpha_0^1)(J_2 - \alpha_0^2)}\right)^{1/2}. \tag{3.6}$$

In Fig. 4 we plot R/b as a function of L for some specific decay modes of the resonances on $\mathfrak{L}_1^N$,

$$\mathfrak{L}_J^N \to \mathfrak{L}_{J-L}^U + \pi, \tag{3.7a}$$

$$\mathfrak{L}_J^N \to \mathfrak{L}_{J-L-1}^N + (\rho, \omega), \tag{3.7b}$$

$$\mathfrak{L}_J^N \to \mathfrak{L}_{J-L+1}^N + \pi, \tag{3.7c}$$

$$\mathfrak{L}_J^N \to \mathfrak{L}_{J-L-2}^N + (A_2, f), \tag{3.7d}$$

$$\mathfrak{L}_J^N \to \mathfrak{D}_{J-L}^U + \pi, \tag{3.7e}$$

$$\mathfrak{L}_J^N \to \mathfrak{L}_{J-L}^N + \gamma. \tag{3.7f}$$

The trajectory $\mathfrak{D}^U$ is the first daughter trajectory of the (π, A_1) trajectory with the same quantum

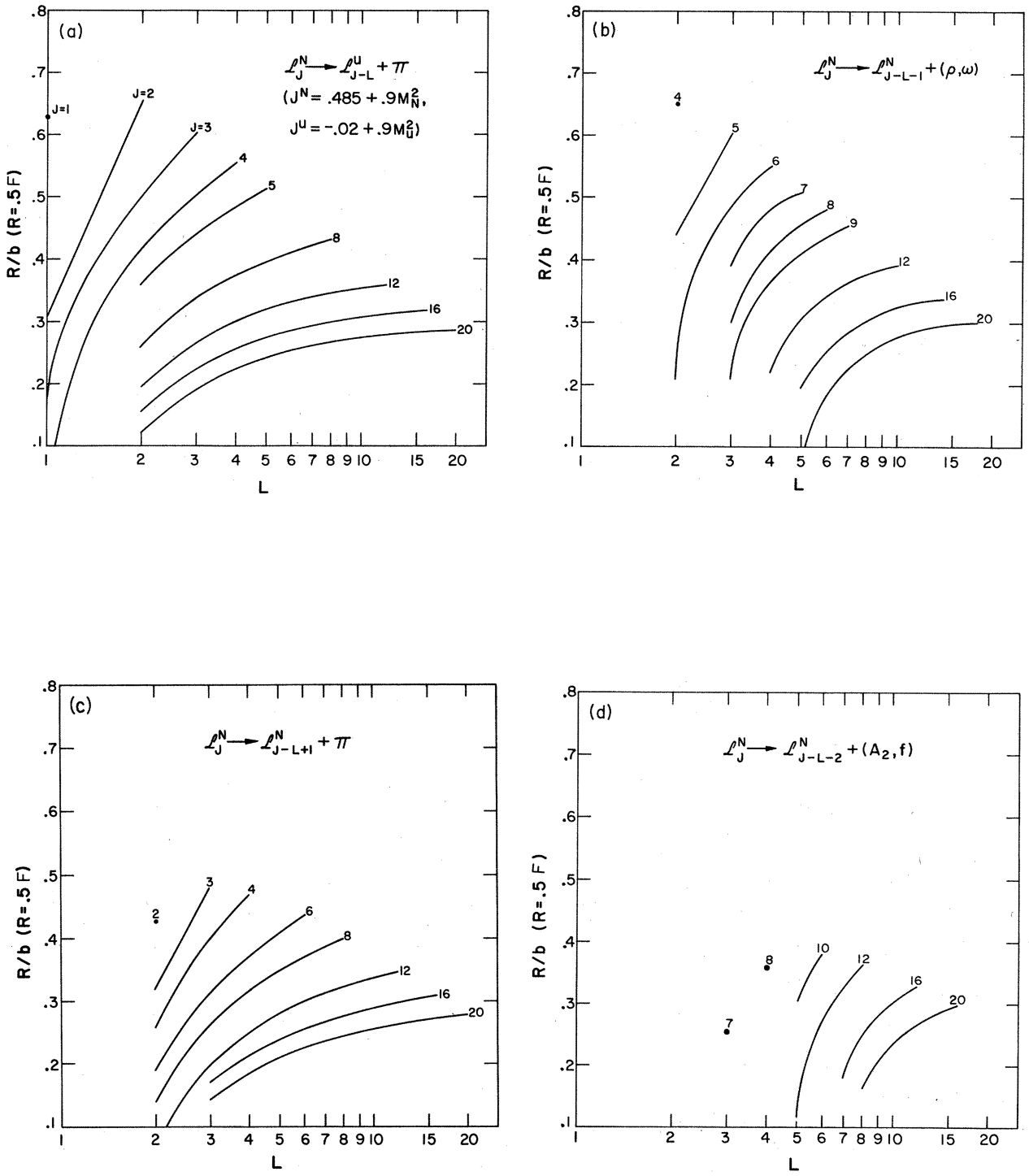

FIG. 4. *(Continued on next page.)*

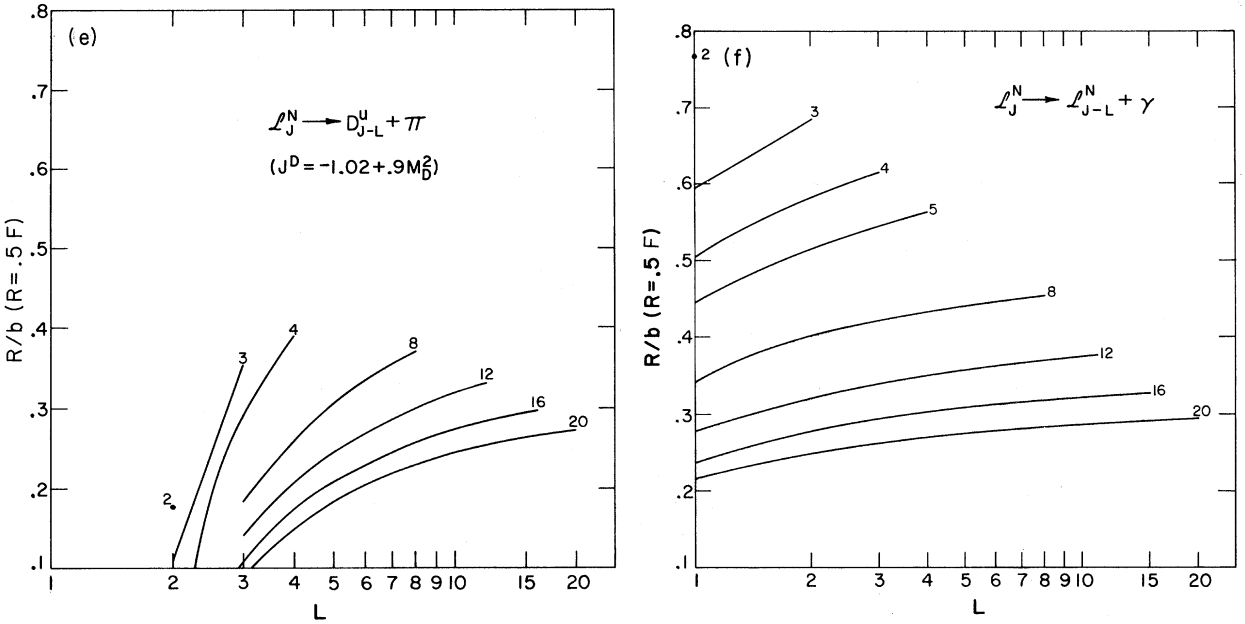

FIG. 4. R/b corresponding to the minimum orbital angular momenta for the decays: (a) $\mathcal{L}^N_J \rightarrow \mathcal{L}^U_{J-L} + \pi$, (b) $\mathcal{L}^N_J \rightarrow \mathcal{L}^N_{J-L-1} + (\rho, \omega)$, (c) $\mathcal{L}^N_J \rightarrow \mathcal{L}^N_{J-L+1} + \pi$, (d) $\mathcal{L}^N_J \rightarrow \mathcal{L}^N_{J-L-2} + (A_2, f)$, (e) $\mathcal{L}^N_J \rightarrow \mathcal{D}^U_{J-L} + \pi$, (f) $\mathcal{L}^N_J \rightarrow \mathcal{L}^N_{J-L} + \gamma$. For convenience, R has been chosen to have the value 0.5 F. The curves are labeled by the corresponding J.

numbers and an intercept one unit less. We have chosen $R = 0.5$ F for convenience in Fig. 4. The scale may be easily varied by the reader. The essential properties of Eq. (3.6) can be seen in the figures, as will be developed in the discussion below.

Recall that the maximum L for any J corresponds to the minimum value of J_1 (J_2 is fixed for each reaction). We also note that the α_0's are all of the order unity. For large L and J we therefore have

$$R/b \rightarrow \tfrac{1}{2} M_0 R J^{-1/2}, \quad J, L \gg 1, \tag{3.8}$$

i.e., the curves become flat and the asymptotic value of R/b decreases as $J^{-1/2}$. It will be seen from Fig. 2(a) that the "kinematic width" decreases rapidly with increasing L at fixed R/b. It would therefore appear that centrifugal-barrier considerations would lead to a preference for those decay modes on the nonasymptotic (low L) parts of the curves in Fig. 4. This means that we must therefore consider the dependence of the curves in the low-L region on the intercepts and parities of the trajectories involved.

Consider first the dependence upon α_0^1 by comparing the curves for reactions (3.7a) and (3.7e) in Figs. 4(a) and 4(e), respectively. It will be seen that the increase in the mass squared of one of the decay products by approximately 1 GeV^2 from (3.7a) to (3.7e) increases b substantially on the low-L part of the curve. This is quite reasonable since decays with low L have low Q value,

$$Q = M_0\{(J-\alpha_0)^{1/2} - [J - L + (0,1) - \alpha_0^1]^{1/2} - (J_2 - \alpha_0^2)^{1/2}\}. \tag{3.9}$$

For an interaction radius of 0.5 F we see from Figs. 2(a), 4(a), and 4(e) that the increased value of b resulting from the lowering of the Regge trajectory of one of the decay products results in this case in the suppression of the most favored decay modes by factors of 10 ($J = 4$) to 100 ($J = 16$). This kinematic suppression of decay channels in which one of the particles has more mass than another possible particle with the same quantum numbers is why we have restricted ourselves in the remaining decays considered in (3.7) to decay products on *leading* natural- and unnatural-parity trajectories as being kinematically preferred.

Consider next the dependence upon J_2 of the kinematical width by comparing the curves in Figs. 4(b) and 4(d). It will be seen that, for the same L, the impact parameters for A_2 emission are substantially larger than those for ρ emission. The reason is the smaller Q value for A_2 emission at the same L. From (3.5) we see that the difference

$$Q_b - Q_d = (M_{A_2} - M_\rho) - (M^N_{J-L-1} - M^N_{J-L-2}),$$
$$J - L - 1 > 2$$

is positive because the mass spacing on the linear trajectory $\mathcal{L}^N$ becomes smaller at higher spins. From comparison of Figs. 4(b) and 4(d) with Fig. 2(a), we see that the resulting suppression of the

kinematic width is typically a factor of 50 for an interaction radius of 0.5 F. For this reason we limit ourselves in the remaining reactions to maximally asymmetric decays in which one of the particles is the lowest particle on its trajectory. Reactions (3.7a) through (3.7c) are of this type.

These two reactions differ in the net change of intrinsic parity. As a result of this parity difference for the same value of L, we have a value of J_1 which is less for (3.7a) than (3.7c) by one unit. This more than compensates for the fact that the unnatural-parity trajectory has an intercept one-half unit lower than the natural-parity trajectory with the result that, according to (3.9), (3.7a) has a Q value larger for the same L and J,

$$Q_a - Q_c = [(J - L + 0.515)^{1/2} - (J - L + 0.02)^{1/2}] M_0.$$

The effect, for a radius $R = 0.5$ F, is a preference of (3.7a) by a factor ranging from 3 ($J = 4$) to 10 ($J = 16$).

In making a comparison between (3.7a) and (3.7b), we have a more complicated situation, because neither decay product is held fixed. The lowest L value of J_1 for which the two decay modes compete is $J_1 = 3$. There we have, for the $I = 1$ mesons, competition between the most favored decay modes of each type,

$$g \to \rho + \rho \quad \text{and} \quad g \to \pi\pi.$$

The Q value of the first channel is much less than that of the second, but so is the orbital angular momentum. Furthermore, because the particles in the first channel are nonrelativistic, they have a higher ratio of c.m. momentum to Q value than do the particles in the second channel. The net effect is that the decay modes (3.7a) and (3.7b) are about equally preferred kinematically for an interaction radius of 0.5 F and J_1 below 8. At higher values of J_1, the Q value advantage of the decay (3.7a) becomes the most important factor, and this decay is more and more favored.

Thus, we have established the following kinematical preferences among energetically allowed two-body decay channels of high-spin mesons on the leading trajectory, assuming trajectories are approximately linear:

(i) Channels with low L are preferred.

(ii) Decays to particles on the highest possible trajectories with a specified natural or unnatural parity are preferred.

(iii) "Cascade" decays with one of the decay particles being the lowest-mass particle on its trajectory are preferred.

(iv) At high J the cascade decay involving the emission of the lightest possible particle is preferred.

(v) It turns out that the kinematically preferred strong decay mode of the leading nonstrange meson trajectory is at high J by pion emission to the leading unnatural-parity meson trajectory when allowed by G parity, and to the leading natural-parity trajectory otherwise. Mesons on the unnatural-parity trajectory will, in turn, prefer to decay via pion emission to the leading natural-parity trajectory.

Finally, we consider the competition of parity-favored electric multipole emission[16] with the preferred strong cascade at high J. It will be seen by a comparison of Figs. 4(f) and 4(a) with Fig. 2(a) that, for an interaction radius of 0.5 F, photon emission is kinematically enhanced over pion emission by about a factor of 100 at $J = 20$. In this case, however, we expect that the reduced width for γ emission must be down by a considerable factor from that for pion emission. To estimate this factor we have compared the parity-favored allowed electric multipole decay widths[17]

$$\Gamma_{N\gamma}(N_{3/2-}(1520)) = 0.55 \text{ MeV},$$

$$\Gamma_{N\gamma}(N_{5/2+}(1688)) = 0.22 \text{ MeV},$$

with the pionic decay widths of the same resonances[12]

$$\Gamma_{N\pi}(N_{3/2-}(1520)) = 65 \text{ MeV},$$

$$\Gamma_{N\pi}(N_{5/2+}(1688)) = 84 \text{ MeV}.$$

For a plausible interaction radius of 0.7 F, the electromagnetic widths are enhanced over the corresponding pionic emission widths by about a factor of 3 in these examples. This means that the reduced widths for photon emission are a factor of about 0.002 or α/π smaller than those for pion emission. For an interaction radius of about 0.5 F for the leading-trajectory meson resonances, we would therefore expect, on the basis of these simple considerations, that strong decays would still dominate over electromagnetic decays at $J = 20$.

Statements about the J dependence of the *total widths* are much more sensitive to the interaction radius than statements about the relative importance of the various possible decay modes. We therefore will not add here to the discussions of these matters which have already appeared in the literature.[14,1-3] The reader may, of course, take his own prejudices about the dependence of the various reduced widths on the decay, the values of the interaction radii in various decay channels, and the possible dependence of the interaction radii on J to obtain a more detailed and quantitative picture of the decay schemes of the high-spin mesons.

Veneziano-Model Results

Chan and Tsou[3] have calculated the partial widths of the mesons on the leading trajectory of a Veneziano amplitude in which the leading trajectory has an intercept -0.02 and a slope of 1 $(\mathrm{GeV}/c)^{-2}$. The lowest-mass particle on the leading trajectory is a scalar meson with a mass about equal to that of the pion.

The results which these authors obtain correspond qualitatively with what we would expect on the basis of centrifugal-barrier considerations *with a J-dependent interaction radius.*

We get a rather good quantitative fit to their results for the cascade widths for the emission of the scalar pion if we take the interaction radius to grow roughly as $J^{1/2}$ or, almost equivalently, as the decaying resonance mass:

$$J=3, \quad R\approx 0.5 \text{ F}, \qquad J=8, \quad R\approx 0.75 \text{ F}, \qquad J=15, \quad R\approx 1.0 \text{ F}. \tag{3.10}$$

The interaction radius is allowed to grow so rapidly by the Veneziano model because arbitrarily-high-spin mesons are exchanged in this model. Since the strength of the interaction associated with the exchange of a particle with spin J_x increases as s^{J_x}, where s is the c.m. energy squared in a two-body channel, the associated Yukawa potential will grow stronger and stronger at any fixed radius as s increases, and hence the radius outside of which the interactions may be neglected must also increase.

Decay of Mesons on Nonleading Trajectories

We have seen above that the decays of high-spin mesons on leading trajectories are substantially suppressed by centrifugal-barrier effects. As soon as we deal with mesons on nonleading trajectories, these supressing effects are considerably reduced, however. In Fig. 5 we illustrate this fact by plotting some sample R/b curves for decays of spin 4, 8, and 16 resonances on a "daughter" trajectory $\mathfrak{D}^N$ with the same quantum numbers as the leading natural-parity meson trajectory but with an intercept one unit down. The decays considered are to the final state in (3.7a).

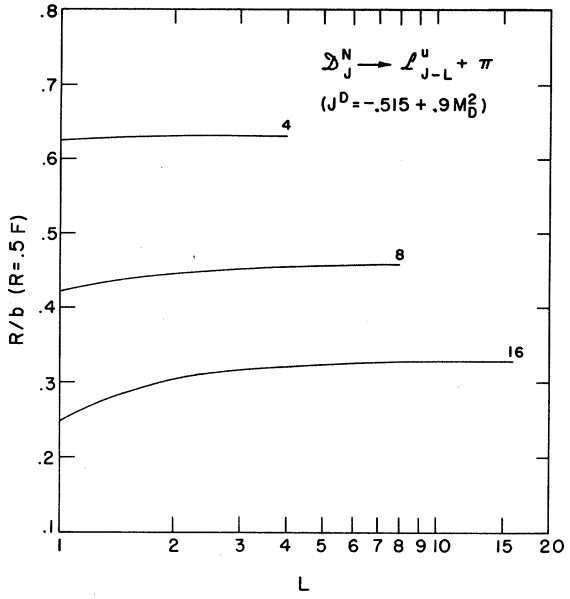

FIG. 5. R/b corresponding to the minimum orbital angular momenta for the decays $\mathfrak{D}^N_J \rightarrow \mathcal{L}^U_{J-L} + \pi$. The curves are labeled by the corresponding J.

From a comparison of Figs. 4(a) and 5 we see clearly the effect of the increased Q value in going from the decay of a resonance on the leading trajectory to the decay into the same final state of a resonance with the same spin on the daughter trajectory. The major effect is to reduce substantially the impact parameters associated with the dominant low-L, low-Q-value decays. For an interaction radius of 0.5 F the effect is to enhance these decay modes by a factor of about 3 for $J=4$, 10 for $J=8$, and 30 for $J=16$. (For $J=1, 2, 3$ s-wave decay channels are available to the daughter resonances.)

In view of these considerations, we expect such resonances to be considerably broader than the corresponding resonances on the parent trajectories. Thus, for example, the large width of the $\pi\pi$ enhancement ($M=1550$ MeV/c^2, $\Gamma=500$ MeV) seen in coherent photoproduction off carbon[18] would not be surprising on kinematical grounds for a ρ-

Table III. Centrifugal-barrier effects in two decay channels of the $\rho_3(1700)$.

Channel	L	$q_{\mathrm{c.m.}}$ (GeV/c)	b (F)	$0.5\left(\frac{1}{b} \pm \frac{\Gamma}{2}\frac{\partial(1/b)}{\partial W}\right)$ $(\mathrm{F}^{-1})^a$
$\pi\pi$	3	0.84	0.81	0.61 ± 0.028
$\pi A_2(1300)$	2	0.33	1.47	0.34 ± 0.066

[a] $\Gamma=0.15$ GeV.

like meson on a low-lying trajectory. On the other hand, the narrow width of the enhancement observed[19] in the formation reaction $\bar{p}p \to K_S^0 K_L^0$ ($M = 1968$ MeV/c^2, $\Gamma = 35$ MeV) is surprising on kinematic grounds for a ρ-like meson. A dynamical reason would have to be invoked for this narrow width if this resonance and its quantum numbers are confirmed. Chan and Tsou found in their Veneziano model that the total widths on the "first daughter" trajectory were about a factor of 5 larger than those on the leading trajectory. The fact that this ratio stays fairly constant as a function of J is in accord with the effective interaction radius for the first daughter trajectory also growing roughly linearly with the decaying resonance mass.

IV. MULTICHANNEL EFFECTS ON RESONANCE SHAPES

The point which we wish to make in this section is one which we have made before.[20] It is simply that the centrifugal-barrier penetration factor in one decay channel of a high-spin resonance may vary more rapidly with energy than that in another with the result that the shape of the resonance may be somewhat different in different channels.

Consider, for example, the decay of the $J^P = 3^-$ recurrence of the ρ, the $\rho_3(1700)$ into the $\pi\pi$ and $\pi A_2(1300)$ channels. If this meson had a width of the order of 150 MeV, comparable to the candidates $g(1670)$ and $\rho_N(1700)$, one would expect to see the mass peak in the πA_2 channel at a higher mass than in the $\pi\pi$ channel. The reason is quite simple, as may be seen from Table III: We see there that both the impact parameter and its fractional variation across the resonance width are larger in the πA_2 than in the $\pi\pi$ channel. It will be seen from Fig. 2(a) that an obvious consequence of these two facts is that the variation with energy of the kinematic width of the ρ_3 will be much larger in the πA_2 than the $\pi\pi$ channel. Thus, for a reasonable interaction radius of 0.5 F, the kinematic width changes by a factor of 3.5 in the πA_2 channel from a half-width below resonance to a half-width above resonance, while the kinematic width in the $\pi\pi$ channel changes only by a factor of 1.6. As a consequence, we expect the ratio of πA_2 to $\pi\pi$ decay probabilities to increase by almost a factor of 2 from the resonance energy to a half-width above resonance. This means that, if the $\pi\pi$ decay probability has decreased to about one-half its maximum value at $W = M_0 + \Gamma/2$, the decay probability in the πA_2 channel will have roughly the same value at that energy as it has at resonance ($W = M_0$), i.e., the mass peak in the πA_2 channel has been shifted by almost $\Gamma/4$ higher in energy than the mass peak in the $\pi\pi$ channel.

It may be that these results are directly applicable to the experimental situation in that there are 2π and 4π enhancements at masses 1660 and 1710 MeV/c^2, respectively, which might in fact both be manifestations of the ρ_3 with the 4π enhancement shifted up in mass by centrifugal-barrier effects such as those considered here. Another possible application might be the $f\pi$ and $\omega\pi\pi$ enhancements observed at 1640 and 1690 MeV/c^2, respectively, which might both be decay modes of the same $J^{PG} = 2^{--}$ particle with the enhancement in the $\omega\pi\pi$ channel being shifted up above the s-wave $f\pi$ enhancement by centrifugal-barrier effects.[8] Even if both these applications turn out to be incorrect they should indicate to us what we should expect as we get into the realm of the high-spin resonances.

The kinematic shifting of the mass peak associated with a resonance in one channel relative to that in another by a significant fraction of the resonance width is apparently a characteristic unique to high-spin resonances. The decay channels of the more familiar resonances with $L = 1, 2$ do not have such large kinematical differences between decay channels.

V. CENTRIFUGAL-BARRIER EFFECTS IN FORMATION AND PRODUCTION EXPERIMENTS

The same centrifugal-barrier effects which make difficult the decay of high-spin meson resonances on a leading linear trajectory make difficult the production of such resonances in formation and peripheral reactions.

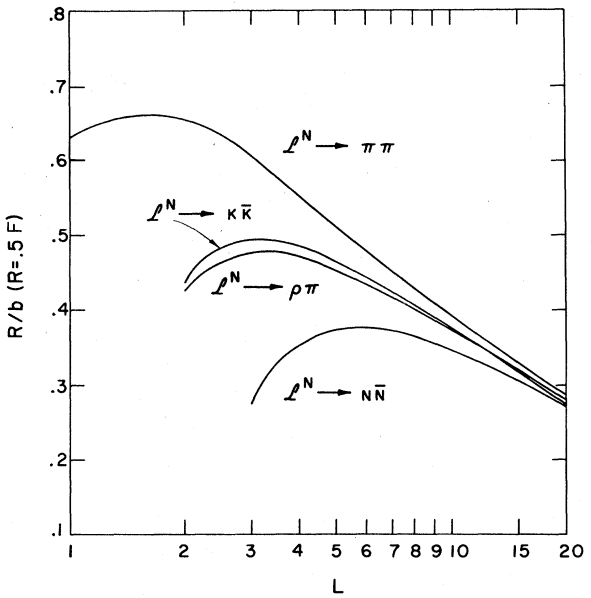

FIG. 6. R/b for corresponding to the mimimum orbital angular momenta for the decays $\mathcal{L}^N \to \pi\pi$, $K\bar{K}$, $\pi\rho$, $N\bar{N}$.

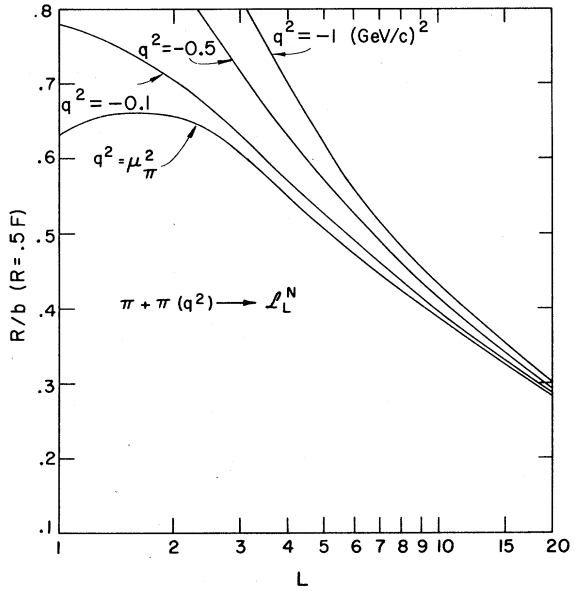

FIG. 7. R/b corresponding to the orbital angular momenta for the decays $\mathcal{L}_L^N \to \pi\pi$ for various values of q^2, one of the pion 4-momenta squared. (The other pion is on its mass shell.)

In Fig. 6 we show plots of R/b for the formation and peripheral reaction channels $\pi\pi$, $K\bar{K}$, $\pi\rho$, $N\bar{N}$, for the production of mesons on the leading natural-parity trajectory. From a comparison with Fig. 2(a) it will be seen that, for a value of $R = 0.5$ F, there is a precipitous drop of the partial widths with increasing J. Even if the interaction radius were to increase as $J^{1/2}$, the partial widths would decrease by about a factor of 1000 for the $\pi\pi$ channel and 100 for the $N\bar{N}$ channel from $J = 4$ to $J = 16$. Chan and Tsou[3] found a corresponding decrease by about a factor of 1000 in the decay of their leading trajectory into two scalar particles with the mass of the pion. In fact in a calculation more directly relevant to the present considerations, the production cross section of mesons on the leading trajectory in the Veneziano model, Tsou finds[21] that they are produced predominantly by "pion" exchange at high energy and that the cross section for production of $J = 15$ resonances is about a factor of 1000 down from that for production of a resonance with $J = 1$.

It is interesting to note that the kinematic width into the $\pi\pi$ channel on the leading trajectory peaks at the $\rho(765)$ and $f(1250)$, and that for the $K\bar{K}$ and $\rho\pi$ channels peaks (with value about three times smaller for $R = 0.5$ F) at $A_2(1300)$ and $g(1700)$, and that into the $N\bar{N}$ channel (at a value about 100 times smaller for $R = 0.5$ F) at $J\ (= L + 1) = 4, 5, 6$ ($M = 1.98, 2.24, 2.48$ GeV/c^2). These results are not inconsistent with our knowledge of the qualitative trend of the experimental widths. The small peak values of the partial widths into the $N\bar{N}$ channel may account for the fact that little information has been developed about leading mesonic resonances from elastic $N\bar{N}$ scattering.

The rapid increase of b with J in the elastic and peripheral reaction channels shown in Fig. 6 leads us to suspect that high-spin mesons on leading trajectories may be exceedingly hard to produce and study by formation or peripheral reactions. In Fig. 7 we show, in the example of the $\pi\pi$ channel, that this situation is not substantially ameliorated by the fact that one of the pions is virtual and has negative (mass)^2. One may hope to learn more about resonances on *nonleading* trajectories in these reactions at higher masses, however. This has been emphasized by Cline[22] who has pointed out in particular that $N\bar{N}$ reactions near threshold may provide expecially favorable conditions for studying the formation of low-spin resonances of about 2-GeV/c^2 mass.

If we wish to study high-spin leading-trajectory mesons, there are at least two other possible ways in which they might be produced. One is as the favored decay products of more copiously produced relatively wide high-mass resonances on nonleading trajectories. The second possibility is suggested by Walker's proposal[23] for the production of *high-mass* resonances by successively higher excitation through multiple scattering of an incident particle in a nucleus. A quantitative estimate of the cross section for the excitation of an incident particle to high spin by this process is currently under way by one of the authors (F.v.H.) in collaboration with James Trefil.

ACKNOWLEDGMENTS

This work was initiated while the authors were at the Lawrence Radiation Laboratory at Berkeley. One of us (F.v.H.) would like to express his appreciation to Geoffrey Chew and the rest of the Theoretical Group for their hospitality during the academic year 1969–70. We would also like to thank Paul Auvil, Chan Hong-Mo, David Cline, David Garelick, Janos Kirz, Dennis Sivers, and William Walker for stimulation and suggestions.

APPENDIX: PROPERTIES OF SPHERICAL HANKEL FUNCTIONS

Spherical Bessel and Hankel functions are customarily defined[24,25] in terms of ordinary Bessel functions of half-odd-integer order as follows:

$$j_l(x) \equiv (\pi/2x)^{1/2} J_{l+1/2}(x), \tag{A1}$$

$$n_l(x) \equiv (\pi/2x)^{1/2} N_{l+1/2}(x), \tag{A2}$$

$$h_l^{(1,2)}(x) \equiv (\pi/2x)^{1/2}[J_{l+1/2}(x) \pm iN_{l+1/2}(x)]. \tag{A3}$$

For real values of x, $h_l^{(1)}(x) = [h_l^{(2)}(x)]^*$. The explicit forms of the first three spherical Hankel functions are

$$h_0^{(1)}(x) = e^{ix}/ix, \tag{A4}$$

$$h_1^{(1)}(x) = -e^{ix}(1 + i/x)/x, \tag{A5}$$

$$h_2^{(1)}(x) = ie^{ix}(1 + 3i/x - 3/x^2)/x. \tag{A6}$$

The asymptotic behavior of the spherical Hankel functions for small arguments $x \ll l$ may be inferred from the forms for the spherical Bessel functions

$$j_l(x) \to x^l/(2l+1)!!, \tag{A7}$$

$$n_l(x) \to -(2l-1)!!x^{-l-1}, \tag{A8}$$

where the double factorial is defined as

$$x!! = x(x-2)(x-4)\cdots. \tag{A9}$$

For large arguments $x \gg l$ the limit is

$$h_l^{(1)}(x) \to -ie^{i(x - l\pi/2)}/x. \tag{A10}$$

The spherical Bessel or Hankel functions satisfy a recursion relation,

$$[(2l+1)/x]\, Z_l(x) = Z_{l-1}(x) + Z_{l+1}(x), \tag{A11}$$

where $Z_l(x)$ is any one of $j_l(x)$, $n_l(x)$, $h_l^{(1)}(x)$, $h_l^{(2)}(x)$.

A power-series expansion useful for computation is

$$h_l^{(1)}(x) = (-i/x)e^{i(x - l\pi/2)} \sum_{k=0}^{l} (-1)^k \frac{(l+k)!}{k!(l-k)!}(2ix)^{-k}. \tag{A12}$$

---

*Work performed partially under the auspices of the U. S. Atomic Energy Commission.

†Alfred P. Sloan Foundation Fellow, 1969–1970.

‡Research supported in part by the U. S. Atomic Energy Commission under Contract No. AT(30-1)-3668 B.

[1]R. C. Brower and John Harte, Phys. Rev. 164, 1841 (1967).

[2]Hyman Goldberg, Phys. Rev. Letters 21, 778 (1968).

[3]Chan Hong-Mo and Tsou Sheung Tsun, Phys. Rev. D 4, 156 (1971).

[4]H. Feshbach, D. C. Peaslee, and V. F. Weisskopf, Phys. Rev. 71, 145 (1947).

[5]This transmission coefficient differs from the corresponding coefficient defined for nuclear applications by J. Blatt and V. F. Weisskopf, *Theoretical Nuclear Physics* (Wiley, New York, 1952), p. 361, because we do not know enough about the dynamics within the interaction radius to estimate the reflection from the inside "wall" of the centrifugal barrier. Aside from an extra factor of $2M/R$ in the kinematic factor extracted, the Blatt-Weisskopf definition (p. 390) of the reduced width for neutron emission in nuclear physics does agree with ours.

[6]Shu-Yuan Chu and A. W. Hendry, Phys. Rev. D 4, 2743 (1971).

[7]Experimental numbers taken from Particle Data Group, Rev. Mod. Phys. 43, S1 (1971).

[8]J. D. Jackson, Nuovo Cimento 34, 1644 (1964).

[9]Angela Barbaro-Galtieri, Advan. Particle Phys. 2, 175 (1968).

[10]See, e.g., the compilation on πn partial-wave amplitudes by the Particle Data Group, LRL Report No. UCRL-20030, 1970 (unpublished).

[11]See, e.g., the discussion of the case of the P_{11} phase shift by George R. Bart and Robert L. Warnock, Phys. Rev. Letters 22, 1081 (1969). A nice discussion of the physics involved was presented in a talk by R. H. Dalitz to the Conference on Hyperon Resonances at Duke University, 1970 [Rutherford Report No. HR-70-003 (unpublished)].

[12]See, e.g., M. Goldberg, J. Leitner, R. Musto, and L. O'Raifeartaigh, Nuovo Cimento 45A, 169 (1966); D. E. Plane, P. Baillon, C. Bricman, M. Ferro-Luzzi, J. Meyer, E. Pagiola, N. Schmitz, E. Burkhardt, H. Filthuth, E. Kluge, H. Oberlack, R. Barloutaud, P. Granet, J. P. Porte, and J. Prevost, Nucl. Phys. B22, 93 (1970).

[13]M. N. Focacci, W. Kienzle, B. Levart, B. C. Maglić, and M. Martin, Phys. Rev. Letters 17, 890 (1966); R. Baud, H. Benz, B. Bosnjokovic, D. R. Botterill, G. Kamgaard, M. N. Focacci, W. Keinzle, R. Klanner, C. Lechanoine, M. Martin, C. Nef, P. Schübelin, and A. Weitsch, Phys. Letters 30B, 129 (1969); R. Baud, H. Benz, B. Bosnjokovic, D. R. Botterill, G. Damgaard, M. N. Focacci, W. Kienzle, R. Klanner, C. Lechanoine, M. Martin, C. Nef, V. Roinishvili, P. Schübelin, A. Weitsch, and H. Jöstlein, *ibid.* 31B, 549 (1970).

[14]R. H. Dalitz, in *Proceedings of the Thirteenth International Conference on High Energy Physics, Berkeley, 1966* (Univ. of California Press, Berkeley, Calif., 1967), p. 215.

[15]D. Sivers, Phys. Rev. D 3, 2275 (1971).

[16]We use the terminology here of Ref. 5, Chap. XII. It will be seen from their discussion that the transitions (3.7f) are parity-favored and that electric multipole transitions correspond to $L = J - J_1$ or greater while magnetic multipole transitions correspond to $L = J - J_1 + 1$ or greater.

[17]These widths have been calculated from the single-pion photoproduction amplitudes of R. L. Walker, Phys. Rev. 182, 1729 (1969).

[18]H. Alvensleben, U. J. Becker, William K. Bertram, M. Chen, K. J. Cohen, R. T. Edwards, T. M. Knasel, R. Marshall, D. J. Quinn, M. Rohde, G. H. Sanders, H. Schubel, and Samuel C. C. Ting, Phys. Rev. Letters 26, 273 (1971).

[19]A. Benvenuti, D. Cline, R. Rutz, D. D. Reeder, and V. R. Scherer, Phys. Rev. Letters 27, 283 (1971).

[20]C. Quigg and F. von Hippel, in *Experimental Meson Spectroscopy,* edited by C. Baltay and A. H. Rosenfeld (Columbia Univ. Press, New York, 1970), p. 477.

[21]Tsou Sheung Tsun, University of Geneva report, 1971 (unpublished).

[22]David Cline, invited paper at the Zero Gradient Synchrotron Summer Workshop on Meson Spectroscopy, 1971 (unpublished).

[23]W. D. Walker, Phys. Rev. Letters 24, 1143 (1970).
[24]*Handbook of Mathematical Functions*, edited by M. Abramowitz and I. Stegun (U.S. GPO, Washington, D.C., 1964).
[25]I. S. Gradshteyn and I. M. Ryzhik, *Tables of Integrals, Series, and Products* (Academic, New York, 1965).

PHYSICAL REVIEW D VOLUME 5, NUMBER 3 1 FEBRUARY 1972

Prospects for Producing and Detecting a Spinless W Boson in High-Energy Neutrino and Muon Experiments*

M. S. Turner† and B. C. Barish
California Institute of Technology, Pasadena, California 91109
(Received 24 September 1971)

We discuss here the possible production of the hypothetical spin-zero W boson (W_0) recently proposed by T. D. Lee, either through the decay of a directly produced spin-one W (W_1) or by direct production in the reactions $\nu + \mathrm{Fe} \to \mathrm{Fe} + W_0 + \mu$ and $\mu + \mathrm{Fe} \to \mathrm{Fe} + W_0 + \nu$. Theoretical cross sections and differential distributions are presented here for W_1 masses between 2 and 40 GeV/c^2 and W_0 masses between 2 and 8 GeV/c^2 for beam energies from 80 to 300 GeV. We show that assuming nonzero muon mass in the calculations for a neutrino beam, rather than zero muon mass as suggested by Lee, can increase the total theoretical cross section by up to a factor of 1000 if M_1 is greater than $4M_0$ or if the W_1's anomalous magnetic moment is near 1. In general, the production cross sections with incident neutrinos for W_0's are down from those for W_1's by a factor of 20–100, while the cross sections with incident muons are nearly equal. The effects of the W_1's anomalous magnetic moment, W_0 and W_1 mass, and incident energy upon cross sections and distributions are discussed for the coherent and incoherent cases. Possible signatures for detecting a W_0 either in the decay of a W_1 or in a q^2–ν plot in direct production are discussed.

I. INTRODUCTION

In one of a recent series of papers on the weak and electromagnetic interactions (in order to make the weak interaction renormalizable), Lee[1] has hypothesized a spinless W boson of opposite metric, in addition to the usual spin-one W boson.

Eventually, with only a spin-one W, cross sections would exceed the unitarity bound in first order. The propagator for a massive particle of spin one is[2]

$$\frac{-\delta_{\mu\nu} + q_\mu q_\nu / M^2}{q^2 - M^2} . \tag{1}$$

The $q_\mu q_\nu$ term, which is not present in the propagator of a massless spin-one particle (i.e., a photon), is what makes renormalization of the weak interactions impossible. As $|q^2|$ increases, the term

$$\frac{q_\mu q_\nu / M^2}{q^2 - M^2} \tag{2}$$

begins to go like a constant, instead of falling with $|q^2|$.

The effect of introducing an additional spinless W is to change the W propagator and the $W_\nu \to W_\mu \gamma$ electromagnetic vertex function everywhere. The propagator becomes[1]

$$\frac{-\delta_{\mu\nu}}{q^2 - M_1^2} + \frac{q_\mu q_\nu}{M_1^2}\left(\frac{1}{q^2 - M_1^2} - \frac{1}{q^2 - M_0^2}\right), \tag{3}$$

where M_1 is the mass of the spin-one W (W_1) and M_0 is the mass of the spinless W (W_0). The minus sign between the W_1 and W_0 propagators is what is meant by opposite metric and is crucial. The W_0 couples to the divergence of the weak current, as is necessary for relativistically invariant amplitudes. Now, the former bothersome $q_\mu q_\nu$ term goes as

$$\frac{q_\mu q_\nu (M_1^2 - M_0^2)}{M_1^2 (q^2 - M_1^2)(q^2 - M_0^2)}, \tag{4}$$

and for large $|q^2|$'s vanishes as $1/|q^2|$. The W_0 fixes up weak-interaction theory so that it mimics electromagnetic-interaction theory and is renormalizable.

In this paper we address ourselves to the possible detection of a W_0, if it exists. Present experiments at the National Accelerator Laboratory (NAL) are expected to search for the W_1 and it is